

TATSUMI YAMAMOTO\*, HIROYUKI KAWASAKI\*,  
HIDEHIRO KUMAZAWA\*

## RELATIONSHIP BETWEEN THE DISPERSED DROPLET DIAMETER AND THE MEAN POWER INPUT FOR EMULSIFICATION IN SEVERAL TYPES OF MOTIONLESS MIXERS

Continuous emulsification of low-viscosity liquids was investigated with three different types of motionless mixers, i.e., Needle Jetting Mixer (NJM), Kenics Static Mixer® (KSM) and Ramond Supermixer® (RSM). Kerosene and *n*-heptane were used as the continuous phase, in which nonionic surfactant (Span80) was dissolved, and deionized water was the dispersed phase. The size distributions of water droplets in emulsions were normalized by the Sauter mean diameter ( $d_{32}$ ), and then they obeyed a log-normal distribution function with an upper-limit. The correlations of  $d_{32}$  with the mean power input per unit mass of the media within the region where the drop dispersion mainly occurred ( $P_M$ ) were derived. The  $P_M$  levels of these motionless mixers were the same as these of agitation vessel. The slopes of the correlation lines on the  $\log(d_{32}) - \log(P_M)$  correlation chart took almost the same value of  $-0.4$ , which agreed with the value derived from isotropic turbulence law in low-viscosity liquids. As the line for RSM was located below those for NJM and KSM, RSM may be the most energy-efficient device of the three.

### NOMENCLATURE

|                   |   |                     |
|-------------------|---|---------------------|
| $c$               | – numerical constant                            | [–]                 |
| $D_i$             | – inner diameter of Kenics Static Mixer         | [m]                 |
| $D_N$             | – inner diameter of an injection needle         | [m]                 |
| $d_{\max}$        | – maximum diameter of droplets                  | [m]                 |
| $d_{\text{med.}}$ | – median diameter of droplets                   | [m]                 |
| $d_{32}$          | – Sauter mean diameter of droplets              | [m]                 |
| $f$               | – distribution fraction of droplet diameter     | [%/ $\mu\text{m}$ ] |
| $f(d/d_{32})$     | – distribution fraction referring to $d/d_{32}$ | [–]                 |
| $k$               | – numerical constant                            | [–]                 |
| $L_e$             | – effective length of mixing pipe               | [m]                 |

---

\* Department of Life Sciences and Bioengineering, Faculty of Engineering, University of Toyama, 3190 Gofuku, Toyamashi, Toyama 930-8555, Japan. E-mail: yamamoto@eng.u-toyama.ac.jp. Phone number: +81-76-445-6861.

|            |  |                      |
|------------|--|----------------------|
| $l^*$      | – stream directional distance between nozzle top and end of mixing area                                | [m]                  |
| $L_E$      | – effective length of the mixing pipe of Kenics Static Mixer   | [m]                  |
| $n$        | – number of mixing units of Ramond Supermixer  | [–]                  |
| $P_M$      | – mean power input per unit mass within the effective region where the drop dispersion mainly occurred | [W/kg]               |
| $Q$        | – flow rate of fluid   | [m <sup>3</sup> /s]  |
| $r$        | – radial distance from center line   | [m]                  |
| $U$        | – linear velocity of liquid flow   | [m/s]                |
| $U_0$      | – velocity at emergence from the nozzle  | [m/s]                |
| $U_{XC}$   | – axial velocity of jet with distance $X$ downstream from origin                                       | [m/s]                |
| $U_X(r)$   | – longitudinal velocity at distance $r$ measured from centerline of jet                                | [m/s]                |
| $V_E$      | – effective volume in which the dispersion occurs  | [m <sup>3</sup> ]    |
| $V_U$      | – volume of the inner space of the mixing unit of Ramond Supermixer                                    | [m <sup>3</sup> ]    |
| $We$       | – Weber number ( $We = U^2 \cdot D_i \cdot \rho_c / \sigma$ )  | [–]                  |
| $X$        | – distance along direction of fluid flow   | [m]                  |
| $\Delta p$ | – pressure drop of fluid passing through KSM or RSM  | [Pa]                 |
| $\rho_c$   | – density of continuous phase liquid   | [kg/m <sup>3</sup> ] |
| $\rho_m$   | – density of emulsion  | [kg/m <sup>3</sup> ] |
| $\sigma$   | – interfacial tension of liquid  | [N/m]                |
| $\phi$     | – volumetric fraction of the dispersion phase in emulsion  | [–]                  |

## 1. INTRODUCTION

Emulsification is an important unit operation in the wide area of the industrial processes related to foods, medicaments and other industrial products. Finer and more homogenized emulsion has been used for the enhanced functionality and stability. To meet the demand, improvements of such traditional devices as the agitation vessel, flow type mixer (motionless mixer) and mechanical homogenizer (colloid mill) have been made, and new types of devices have been developed, day by day, using various types of driving forces such as high-frequency current, electrostatic force, ultrasonic force and extra-high pressure. On the other hand, previous research regarding the mainstream operation of liquid–liquid dispersion by the mechanical shear force of liquid was done using agitated vessel type equipment. Currently, the research trend is directed towards the motionless mixer with the continuous flow operation. In the chemical process industry, many types of motionless mixers have been used for liquid mixing or emulsification operations. The emulsification technique using the motionless mixer can be readily applied in a waste oil incinerator [1] or in a diesel engine [2], [3] using emulsion combustion for the reduction of harmful components in the exhaust fumes. The motionless mixer attains mixing using the kinetic energy of the fluid as it passes through various types of motionless elements. When two immiscible liquids are subject to the shear force within a motionless mixer, droplets of one phase are produced within the other. The droplet size distributions and their characteristic sizes depend on the flow rates of the liquids, the geometries of the mixers (or the mixer

elements) and the physical properties of the liquids. The dispersed droplet size has an important effect on the stability of emulsion.

In the previous report [4], we presented parallel results of the emulsification of low-viscosity liquid systems with three different types of motionless mixer, i.e., Needle Jetting Mixer (NJM), Kenics Static Mixer<sup>®</sup> (KSM) and Ramond Super-mixer<sup>®</sup> (RSM). NJM is a simple motionless mixer developed by YAMAMOTO et al. [5] for the application in the midget-type in-vehicle emulsification unit for emulsion combustion. KSM is one of popular motionless mixers. RSM is a high performance motionless mixer commercialized by Environmental Science Technology Corporation in Japan. We pointed out the inexpediency of the proposed usually dimensionless correlation of the Sauter mean diameter ( $d_{32}$ ) of water droplets dispersed in emulsion with the Weber number since it is difficult to estimate the characteristic length involved in the dimensionless correlation for the complicated flow path like in the motionless mixers. In our recent short communication [6], the comparison of  $d_{32}$  of dispersed droplet with the mean power input per unit mass of the media within the region where the drop dispersion mainly occurred ( $P_M$ ) proposed by DAVIES [7], [8] was reported.

This article covers the details of the experimental data and the calculation methods described briefly in the previous reports.

## 2. EXPERIMENTAL

### 2.1. DETAILS OF MOTIONLESS MIXERS

NJM has two parallel injection stainless steel needles, from which the organic liquid and water were separately jetted into a small glass mixing chamber as shown in figure 1. The inner diameters of the needles were 0.30, 0.50 and 0.70 mm, and the volume of the mixing chamber was 3.25 cm<sup>3</sup>. KSM (Noritake Co., Inc.) is composed of 21 short stainless steel elements of right- and left-handed helices in a straight stainless steel pipe, whose elements are alternated and oriented so that each leading edge is located at 90° to the trailing edge of the one ahead as shown in figure 2. Here, KSM

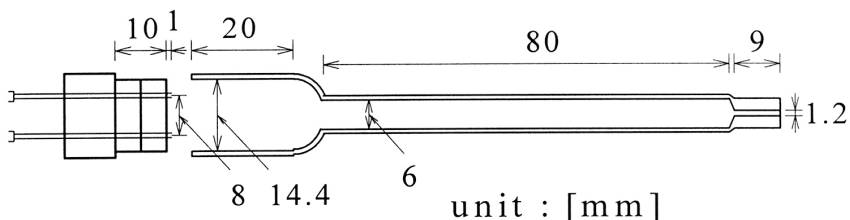
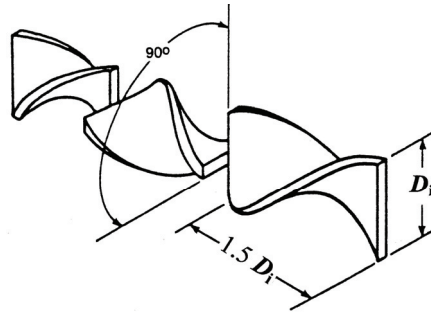


Fig. 1. Configuration on Needle Jetting Mixer



( $D_i$  : inside diameter of pipe)

Fig. 2. Mixing elements of Kenics Static Mixer

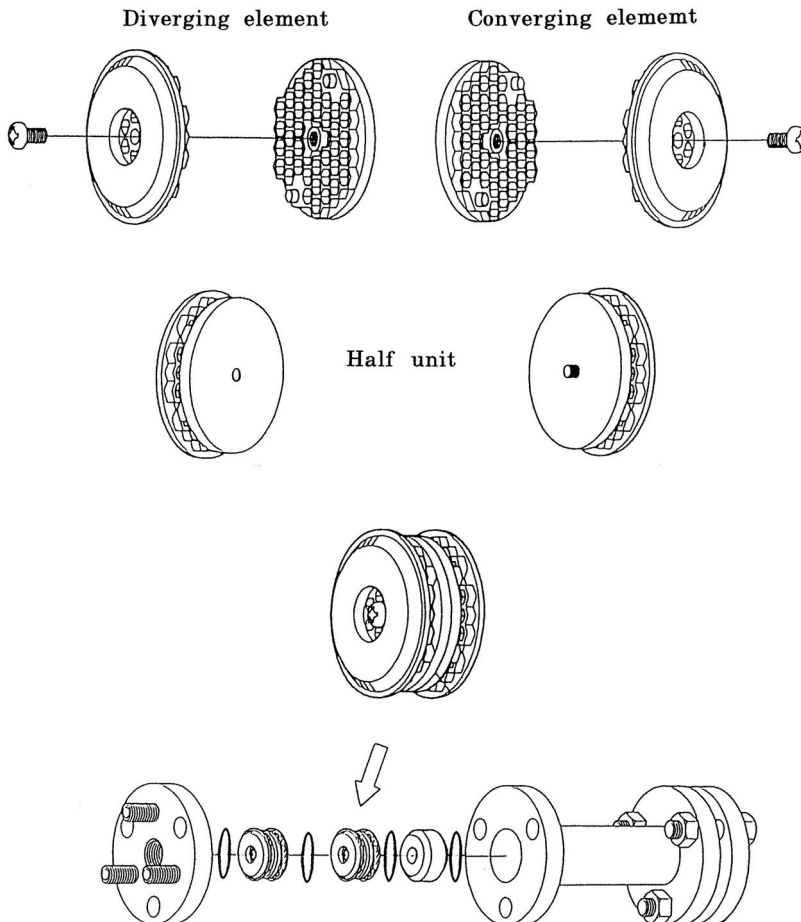


Fig. 3. An outward form and the mixing unit of Ramond Supermixer

with two different diameters, 5.0 and 3.4 mm, were used. RSM (Environmental Science Technology Co., Inc.) is composed of a series of disk-shaped stainless steel units, arranged inside a cylindrical stainless steel casing (the inner diameter is 36 mm), as shown in figure 3. One unit is composed of a pair of diverging and converging elements, and the dimensions of the unit were 20 mm thick and 36 mm in diameter. On the surface of each element, 97 hexagonal cells with 2.2 mm depth are arranged compactly like a honeycomb. When the number of units were changed, a spacer was put in the casing instead of a mixing unit. The capacity of the casing was as big as ten units or spacers.

## 2.2. EMULSIFICATION AND MEASUREMENTS OF PRESSURE DROP

Kerosene (Katayama Chemical Industries Co., Inc.) or *n*-heptane (Kishida Chemical Co., Inc.) were used as the continuous phase, in which nonionic surfactant, Span80 (sorbitan monooleate, Kanto Chemical Co., Inc.), was dissolved in a concentration of 30 kg/m<sup>3</sup> (kerosene) or 10 kg/m<sup>3</sup> (*n*-heptane) which was 10 times the concentration as the critical micelle concentration of Span80, and deionized water used as the dispersed phase. The volumetric fraction of dispersed phase ( $\phi$ ) is changed as follows: 0.26, 0.34, 0.50, 0.66, 0.74 (for NJM), 0.02, 0.1, 0.15, 0.2, 0.3, 0.5, 0.7 (for KSM), and 0.1, 0.3, 0.5 (for RSM). The emulsifications using RSM need the premixing to prepare to various volumetric fractions of the dispersed phase. As the hydrophile–lipophile balance (HLB) of Span80 is 4.3 (GRIFFIN, 1954) [9] or 6.8 (PASQUALI, 2008) [10], the water in oil type emulsion was formed in experimental conditions ( $\phi \leq 0.74$ ). All emulsifications were carried out at a temperature of  $303 \pm 0.5$  K. Table 1 shows the physicochemical properties of the liquids used at 303 K. Water droplet diameters in emulsions were measured by microphotography. Here, the amount of measured droplets in each run was above one thousand droplets. The diameters larger than five-fold of the Sauter mean diameter ( $d_{32}$ ) were neglected [11], because these large droplets must be generated by the coalescence with the instability of dispersed droplet in measurement. Even if there were enormously large droplets, only a few of diameters were neglected. In most of the run, none of the droplets were neglected. The pressure drop of water flow passing RSM was measured with a differential pressure transducer (Type: DP15, Validyne Engineering Co., Inc.) and amplifier (Type: PA501-S, Krone Co., Inc.) system.

Table

Physicochemical properties of liquids at 303 K

| Samples  | Density                     | Viscosity              | Kinematic viscosity       | Interfacial tension to water |
|--|-----------------------------|------------------------|---------------------------|------------------------------|
|  | $\rho$ [kg/m <sup>3</sup> ] | $\mu$ [Pa·s]           | $\nu$ [m <sup>2</sup> /s] | $\sigma$ [N/m]               |
| Water  | 996                         | $0.798 \times 10^{-3}$ | $0.801 \times 10^{-6}$    | –                            |
| Kerosene + Span80 (30 kg/m <sup>3</sup> ) [22]     | 788                         | 1.088                  | 1.377                     | $3.50 \times 10^{-3}$        |
| <i>n</i> -Heptane + Span80 (10 kg/m <sup>3</sup> ) | 678                         | 0.382                  | 0.563                     | 4.20                         |

### 3. RESULTS AND DISCUSSION

#### 3.1. SIZE DISTRIBUTIONS OF WATER DROPLETS IN EMULSION

Typical size distributions of water droplets in emulsion prepared by the motionless mixers are shown in figures 4 to 6 [4], [12], [13]. When the drop size was normalized by Sauter mean diameter ( $d_{32}$ ) for each set of data, all of the data fell on a curve with the same upper-limit on a log-normal probability paper as shown in figures 7 to 9 [4],

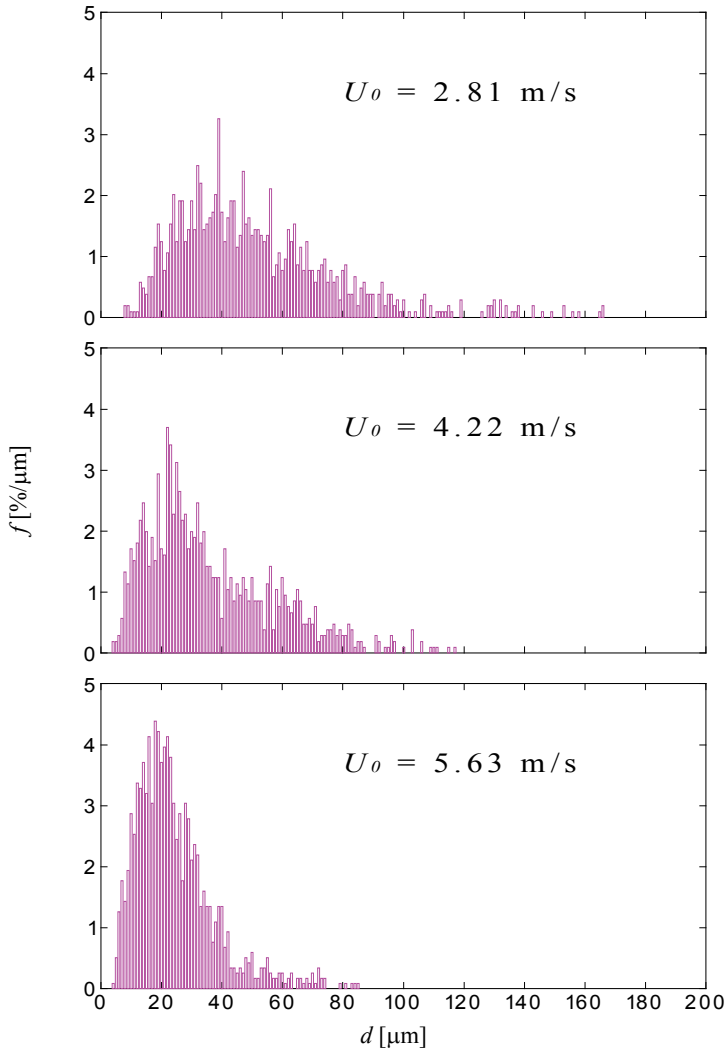


Fig. 4. Droplet diameter distributions in the water-in-kerosene emulsions generated with Needle Jetting Mixer ( $D_{Nd} = D_{Nc} = 0.5$  mm,  $\phi = 0.5$ )

[12], [13]. The linearity of the curve suggested that the normalized drop size distributions roughly followed a log-normal probability function with an upper-limit. The drop size distributions in emulsion prepared by RSM were basically the same as those by NJM and KSM. Figures 10 to 13 [4], [12], [13] show the relationships between the maximum diameter ( $d_{\max}$ ) and  $d_{32}$  of droplets with the three types of mixer and the relationships between the median size ( $d_{\text{med}}$ ) and  $d_{32}$  as well. In these figures, linear dependencies of  $d_{\max}$  and  $d_{\text{med}}$  on  $d_{32}$  are exhibited. The ratios of  $d_{\max}$  to  $d_{32}$  were estimated to be 2.3 for NJM and KSM and 1.9 for RSM, respectively, and the ratios of  $d_{\text{med}}$  to  $d_{32}$  were calculated to be 0.5 for the three types of mixers. The geometric standard deviation calculated from  $d_{\text{med}}/d_{32}$  was evaluated to be 1.7. This means that the size distribution of the emulsions formed by RSM is slightly sharper than those formed by NJM and KSM. But then, for RSM results with 1 or 2 units, the size distributions somewhat broadened. Almost similar results were obtained for water–kerosene and water–heptane systems.

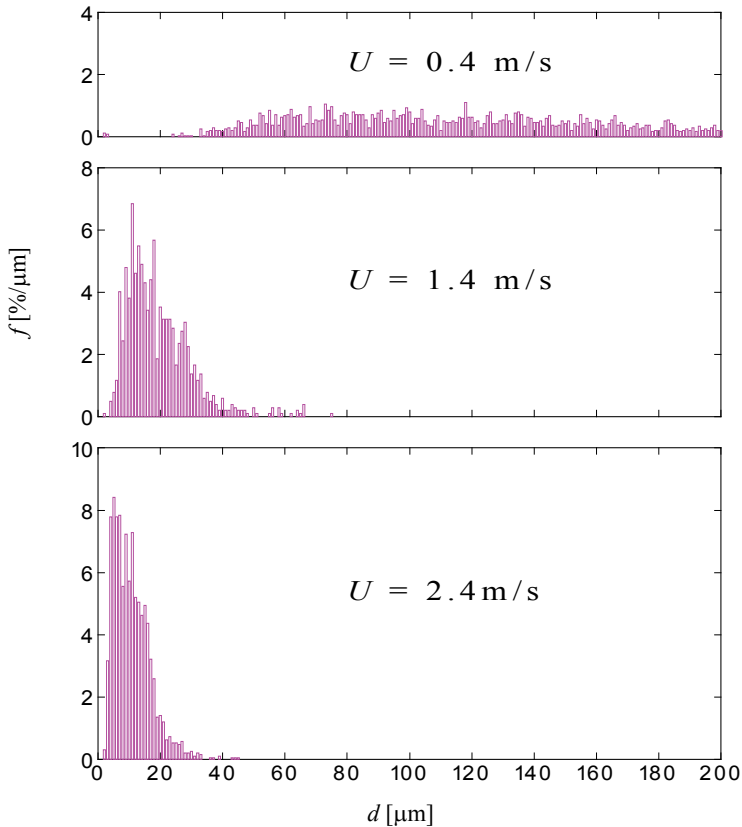


Fig. 5. Droplet diameter distributions in the water-in-kerosene emulsions generated with Kenics Static Mixer ( $D_i = 5$  mm,  $\phi = 0.5$ )

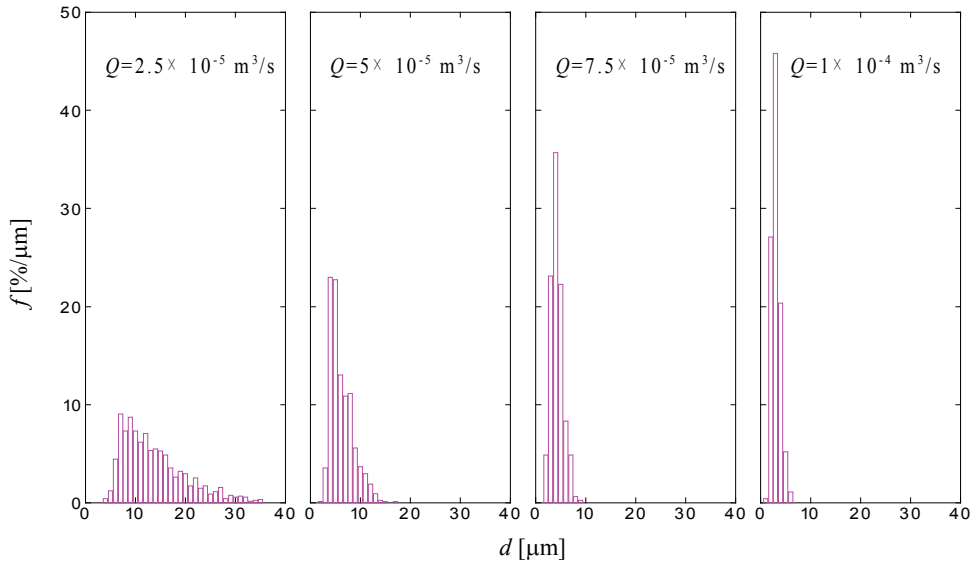


Fig. 6. Droplet diameter distributions in the water-in-kerosene emulsions generated with Ramond Supermixer ( $n = 10$ ,  $\phi = 0.5$ )

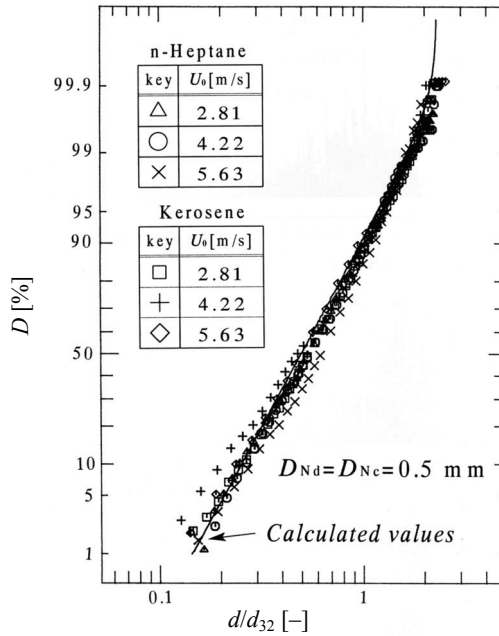


Fig. 7. Cumulative distributions of droplet diameters in the emulsions generated with Needle Jetting Mixer ( $D_{Nd} = D_{Nc} = 0.5$  mm,  $\phi = 0.5$ )



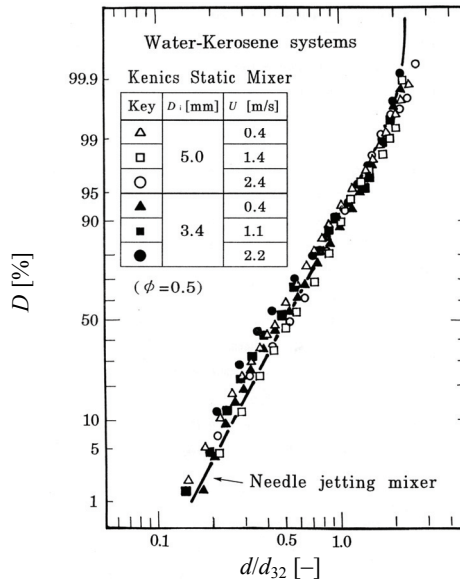


Fig. 8. Cumulative distributions of droplet diameters in the water-in-kerosene emulsions generated with Kenics Static Mixer ( $\phi = 0.5$ )

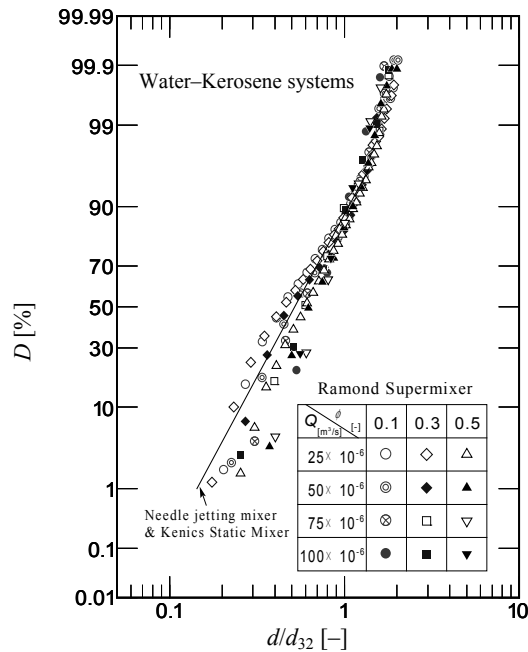


Fig. 9. Cumulative distributions of droplet diameters in the water-in-kerosene emulsions generated with Ramond Supermixer

### 3.2. DEPENDENCIES OF SAUTER MEAN DIAMETER ( $d_{32}$ ) ON OPERATING VARIABLES

The dispersed droplet diameter in emulsion using kerosene as the continuous phase was larger than that using *n*-heptane in all emulsification. The ratio of the mean diameters approximately agreed with the value (1.22) estimated from equation (1) proposed by DAVIES [7], [8] based on the isotropic turbulence law for low-viscosity liquids. Here, Davies remarked that the coefficient  $c$  ranged from 0.5 to 1.0.

$$d_{\max} = c \cdot (\sigma/\rho_c)^{0.6} \cdot P_M^{-0.4}. \quad (1)$$

However, as the dependence of the mean droplet diameter on the operating variables was not the same in each type of mixer, the common rate was not picked out from the data of the mixers. Consequently, the empirical formulas of the Sauter mean diameter ( $d_{32}$ ) derived in the respective mixing devices are listed below.

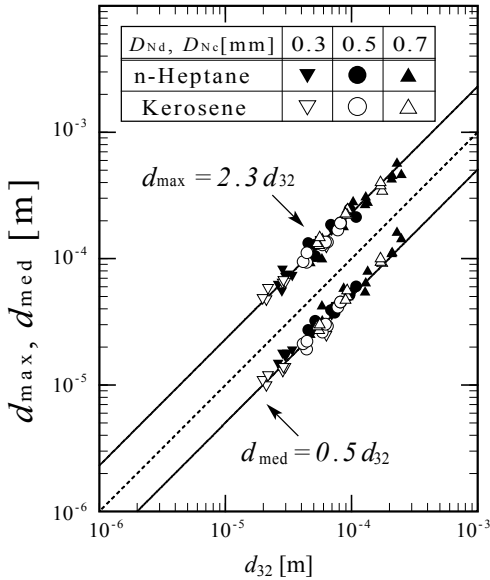


Fig. 10. Relations of  $d_{\max}$  and  $d_{\text{med}}$  versus  $d_{32}$  of water droplets in emulsions generated with Needle Jetting Mixer

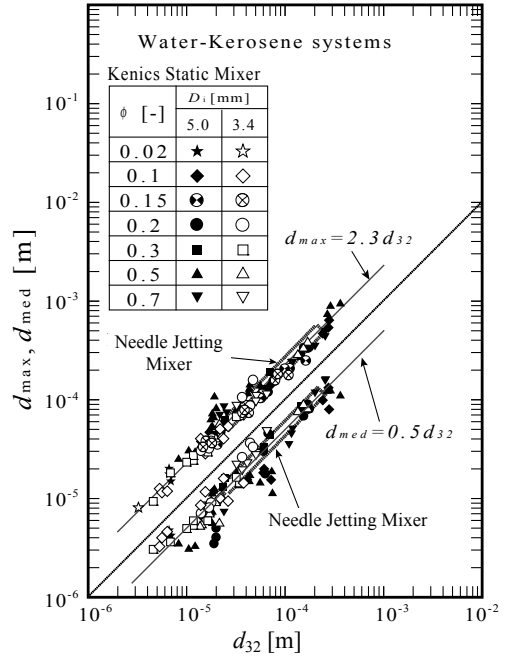


Fig. 11. Relations of  $d_{\max}$  and  $d_{\text{med}}$  versus  $d_{32}$  of water droplets in the water-in-kerosene emulsions generated with Kenics Static Mixer

For NJM ( $\phi = 0.50$ ), (YAMAMOTO et al. [12])

$$d_{32} = 0.0086 \cdot U_0^{-1} \cdot D_N^{-0.35} \cdot (\sigma/\rho_c)^{0.5}. \quad (2)$$

For KSM (BERKAMN and CALABRESE [14], [15], YAMAMOTO et al. [13])

$$d_{32}/D_i = 0.49 \cdot We^{-0.6} = 0.49 \cdot (\sigma/\rho_c)^{0.6} \cdot U^{-1.2} \cdot D_i^{-0.6}, \quad (3)$$

where  $We = U^2 \cdot D_i \cdot \rho_c / \sigma$ .

For RSM ( $3 \leq n \leq 10$ ,  $0.1 \leq \phi \leq 0.5$ ), (YAMAMOTO and KUMAZAWA [16]):

$$d_{32} = 1.47 \times 10^{-7} \cdot (\sigma/\rho_c)^{0.6} \cdot Q^{-1.2} \cdot n^{-0.2}, \quad (4)$$

where  $Q$  is the volumetric flow rate of the fluid mixture,  $n$  is the number of units and  $\phi$  is the volumetric fraction of the dispersed phase in the emulsion flow in RSM.

### 3.3. CORRELATION OF SAUTER MEAN DIAMETER ( $d_{32}$ ) OF DROPLETS WITH THE MEAN POWER INPUT RATE PER UNIT MASS FOR EMULSIFICATION ( $P_M$ )

The dimensionless correlation of the Sauter mean diameter ( $d_{32}$ ) of the dispersed droplets with the Weber number or Reynolds number is usable for the simple flow path device such as KSM [17]. However, for the complicated flow path like the ones in NJM and RSM, the characteristic length involved in the available dimensionless correlation is difficult to estimate. MCMANAMEY [18] showed that the breakup of

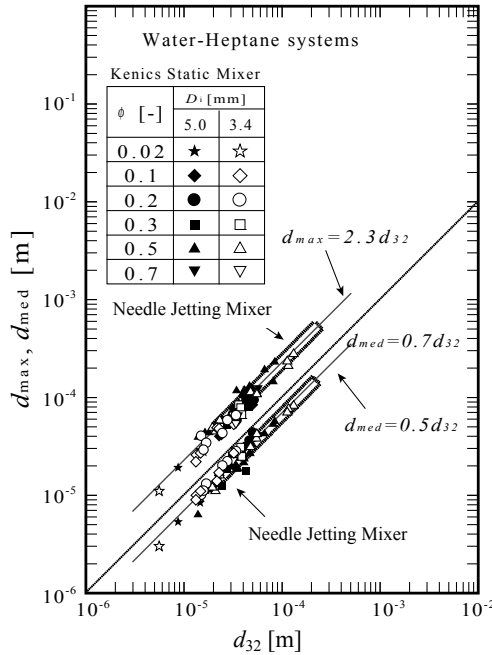


Fig. 12. Relations of  $d_{max}$  and  $d_{med}$  versus  $d_{32}$  of water droplets in the water-in-heptane emulsions generated with Kenics Static Mixer

dispersed droplets occurred in a confined space adjacent to the revolving impeller blade in an agitation vessel. On the basis of the results, DAVIES [7], [8] proposed the correlation of the maximum diameter ( $d_{max}$ ) or Sauter mean diameter ( $d_{32}$ ) of droplets with the mean power inlet rate per unit mass of the media applied in the effective region for emulsification ( $P_M$ ). As an alternative of the correlation of droplet diameter with the Weber number, the correlation with  $P_M$  was useful for the devices having complicated flow paths like NJM and RSM.

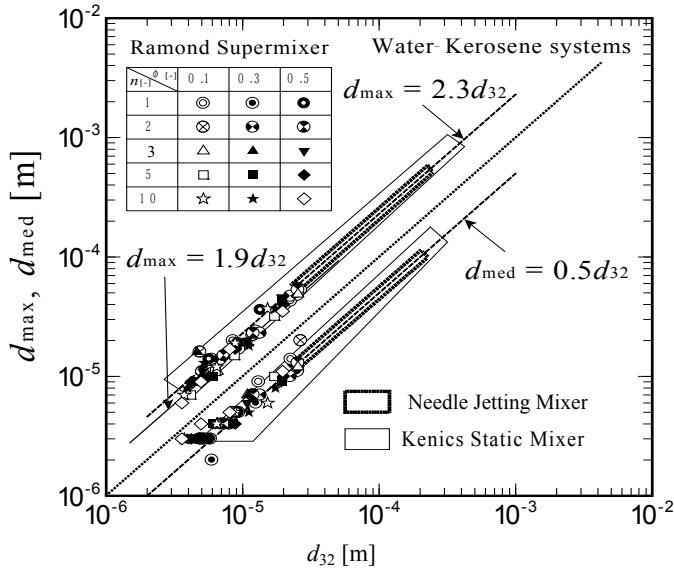


Fig. 13. Relations of  $d_{max}$  and  $d_{med}$  versus  $d_{32}$  of water droplets in the water-in-kerosene emulsions generated with Ramond Supermixer

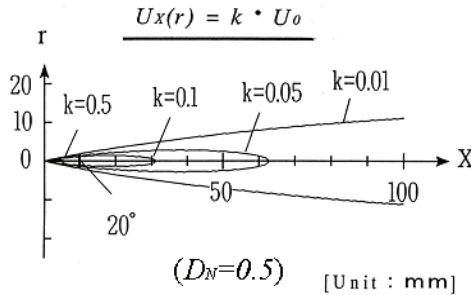


Fig. 14. Free turbulent jet models based on equations (5) to (7)

The effective region available for the emulsification in NJM was estimated using a free jet model as follows [12]. Figure 14 shows a geometric model of an axial sym-

metry and fully developed turbulent jet discharged from a circular nozzle into the stationary fluid. The model was calculated using the following equations [19].

$$\frac{U_{XC}}{U_0} = 6.3 \cdot \frac{D_N}{X}, \quad \left( 7 < \frac{X}{D_N} < 100 \right), \quad (5)$$

$$\log \left( \frac{U_{XC}}{U_{X(r)}} \right) = 40 \cdot \left( \frac{r}{X} \right)^2. \quad (6)$$

Here, it was assumed that the potential core of the jet was vanishingly small, and that the surface of the jet converged to the centre of the nozzle spout. Equation (7) is satisfied inside of the jet in figure 14.

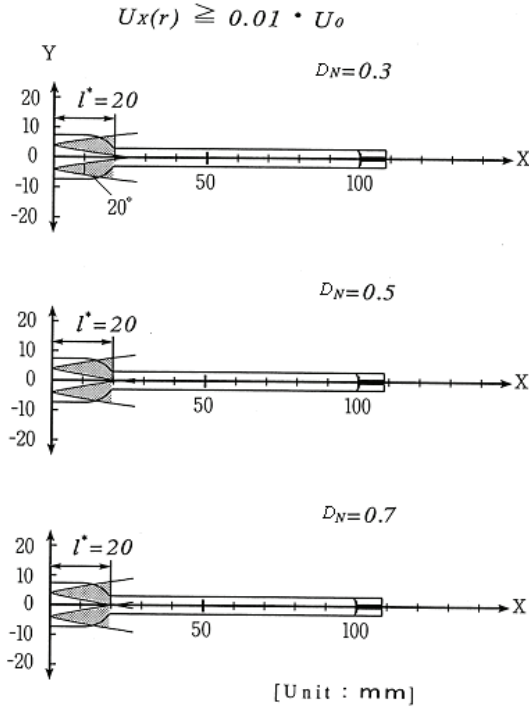


Fig. 15. Plausible sketch of the effective region for drop dispersion in Needle Jetting Mixer

$$U_X(r) \geq k \cdot U_0, \quad (0 < k < 1). \quad (7)$$

The effective region for emulsification in the NJM was assumed to occur within the portion of the jet from the nozzle spout ( $X=0$ ) to  $X=l^*$ . From equation (6),  $r^2$  and the effective volume  $V_E$ , in which the drop dispersion occurred, were derived as follows.

$$r^2 = \frac{1}{40} \left\{ \log \left( \frac{6.3 \cdot D_N}{k} \right) - \log X \right\} \cdot X^2, \quad (8)$$

$$V_E = \int_0^{l^*} \pi \cdot r^2 dX = 2.617 \times 10^{-2} \cdot l^{*3} \left\{ \log \left( \frac{6.3 \cdot D_N}{k \cdot l^*} \right) + 0.1448 \right\}. \quad (9)$$

As the angle of the jet was estimated at  $20^\circ$  based on the earlier study [20] and the photographic observation,  $k = 0.01$  was derived. The jet length  $l^*$  was estimated  $2 \times 10^{-2}$  m for keeping the shape inside the mixing room as shown in figure 15. The  $V_E$  and the mean power inlet rate per unit mass of the media applied in the effective region available for emulsification ( $P_M$ ) are derived as follows:

$$V_E(D_N) = 8 \times 10^{-6} \cdot D_N^{0.45}, \quad (10)$$

$$P_M = \frac{\pi}{8} \cdot \frac{D_N^2}{V_E} \cdot U_0^3. \quad (11)$$

Here, it must be kept in mind that this calculation is based on a rough model limited for low viscosity liquid used in this study.

For KSM, as frictional pressure loss of flow may be almost 50-fold of that in empty circular pipe [17], [21], we estimated that the Fanning's friction factor was 0.5 within our experimental flow range ( $1000 < Re < 14000$ ).  $P_M$  is derived as follows:

$$P_M = \frac{Q \cdot \Delta p}{\rho \cdot V_E} = \frac{AU \cdot (\rho L_E U^2 / D_i)}{\rho V_E} = \frac{U^3}{D_i}. \quad (12)$$

Here,  $L_E$  is the path length of the effective mixing elements and  $D_i$  is the inner diameter of the pipe. However, the effective region for emulsification in KSM is limited within about 10 elements from the inlet with pressure drop caused by the mixing elements [17].

Figure 16 shows the dependence of the pressure drop  $\Delta p$  on the volumetric flow rate of water ( $Q$ ) and the number of units ( $n$ ) in RSM, and we obtained equation (13). As the difference of viscosity between water and emulsion will be small, the measured  $\Delta p$  must be close to that with the emulsion system.

$$\Delta p = 1.9 \times 10^{13} \cdot Q^{1.9} \cdot n^{0.67}. \quad (13)$$

The mean power input per unit mass of media to be mixed within the effective area for emulsification ( $P_M$ ) was calculated as follows:

$$P_M = \frac{Q \cdot \Delta p}{V_U \cdot n \cdot \rho_m} = 1.9 \times 10^{13} \cdot Q^{2.9} \cdot n^{-0.33} \cdot (V_U \rho_m)^{-1}. \quad (14)$$

Here,  $V_U$  and  $\rho_m$  are the inner volume of one unit and the density of emulsion, respectively.

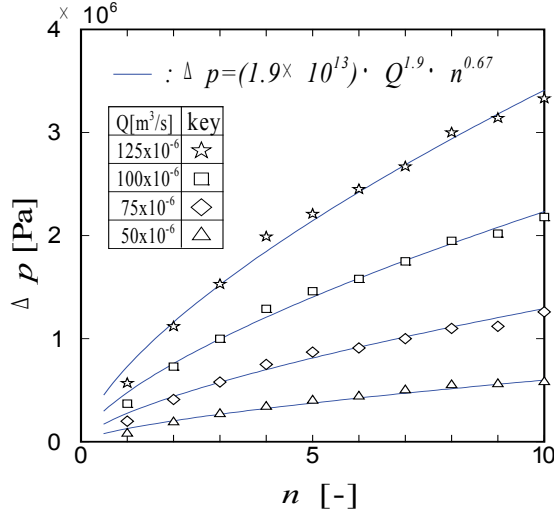


Fig. 16. Relations of  $\Delta p$  versus  $n$  with  $Q$  as a parameter in Ramond Supermixer

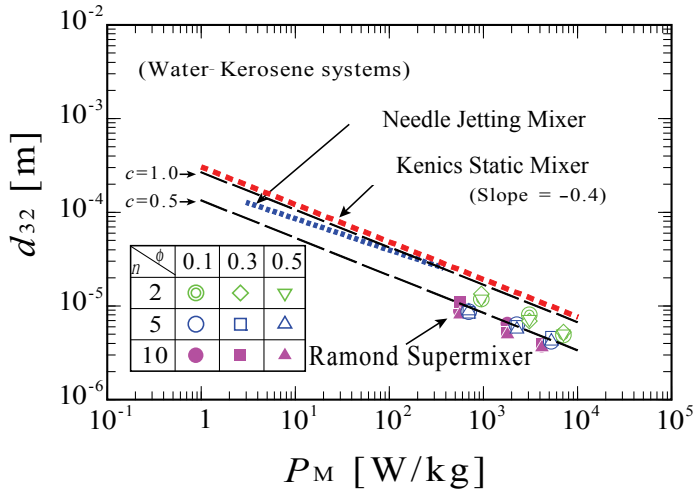


Fig. 17. Correlation of  $d_{32}$  with the mean power input rate per unit mass of the media applied in the effective region for emulsification ( $P_M$ )

Figure 17 shows the correlations of  $d_{32}$  with  $P_M$  for water–kerosene (Span80) systems. Here, it appears that the slopes of the correlation lines of KSM and RSM take

almost the same value of  $-0.4$ . The slope  $-0.4$  agrees with the value expected when the drop breakup should be induced by the turbulent fluctuations of low-viscosity fluids according to DAVIES [7], [8]. As Davies remarked,  $c$  in equation (1) ranged from 0.5 to 1.0, the two broken lines are drawn with substituting 0.5 and 1.0, respectively, into  $c$ . However, in our emulsification conditions, the fully developed turbulence field, where an isotropic turbulence model was assumable, would not come in the mixers. The correlations of  $d_{32}$  with  $P_M$  might merely show the pseudoturbulent dispersion caused by the complicated flow pass in the mixers. In the data of RSM, the effects of volumetric fractions of dispersed phase ( $\phi$ ) did not appear, but the number of units ( $n$ ) had influence on the dispersed drop sizes. In the cases of  $n = 5$  to 10, the plots of RSM are located below the line of  $n = 2$ . In these cases, more efficient emulsification must be attained in RSM.

#### 4. CONCLUSIONS

Continuous emulsifications of low-viscosity liquids were investigated with three different types of motionless mixers i.e., Needle Jetting Mixer (NJM), Kenics Static Mixer<sup>®</sup> (KSM) and Ramond Supermixer<sup>®</sup> (RSM). The size distributions of water droplets normalized by  $d_{32}$  obeyed a log-normal function with an upper-limit. The size distributions of the droplets formed by RSM were slightly sharper than those by NJM and KSM. The slopes of correlation of  $d_{32}$  with the mean power input per unit mass of media within the effective region, where the drop dispersion mainly occurred ( $P_M$ ), were  $-0.4$  for KSM and RSM. The  $P_M$  levels of these motionless mixers were the same as those of agitation vessel in our experimental conditions.

#### REFERENCES

- [1] AL-MAAMARI R.S., SHIGEMOTO N., HIRAYAMA A., SUEYOSHI M.N., *Combustion Properties of Emulsion Fuel Prepared from Heavy Crude Oil in Oman*, J. Chem. Eng. Japan, 2007, 40, 105–107.
- [2] HUSNAWAN M., MASJUKI H.H., MAHLIA T.M.I., SAIFULLAH M.G., *Thermal Analysis of Cylinder Head Carbon Deposits from Single Cylinder Diesel Engine Fuelled by Palm Oil–Diesel Fuel Emulsions*, Applied Energy, 2009, 86, 2107–2113.
- [3] BASHA S.A., GOPAL K.R., JEBARAJ S., *A Review on Biodiesel Production, Combustion, Emissions and Performance*, Renewable and Sustainable Energy Reviews, 2009, 13, 1628–1634.
- [4] YAMAMOTO T., KUMAZAWA H., *Emulsification of Low-Viscosity Liquids with Three Different Types of Motionless Mixer*, Proceedings of the 8th APCChE Congress, Seoul, Korea, 1999, 2153–2156.
- [5] YAMAMOTO T., NISHII K., KAWASAKI H., TANAKA H., *Formation of W/O Emulsions by Twin-Needle Jet Disperser*, Kagaku Kogaku Ronbunshu (Collected Papers of Chemical Engineering, Japanese document), 1995, 21, 944–947.
- [6] YAMAMOTO T., KAWASAKI H., KUMAZAWA H., *Relationship between the Dispersed Droplet Diameter and the Mean Power Input for Emulsification in Three Different Types of Motionless Mixer*, J. Chem. Eng. Japan, 2007, 40, 673–678.



- 
- [7] DAVIES J.T., *Drop Sizes of Emulsions Related to Turbulent Energy Dissipation Rates*, Chem. Eng. Sci., 1985, 40, 839–842.
- [8] DAVIES J.T., *A Physical Interpretation of Drop Sizes in Homogenizers and Agitated Tanks, Including the Dispersion of Viscous Oils*, Chem. Eng. Sci., 1987, 42, 1671–1676.
- [9] GRIFFIN W.C., *Calculation of HLB Values of Non-Ionic Surfactants*, J. Soc. Cosmet. Chem., 1954, 5, 249–256.
- [10] PASQUALI R.C. et al., *Some Considerations about the Hydrophilic–Lipophilic Balance System*, International Journal of Pharmaceutics, 2008, 356, 44–51.
- [11] TAKAHASHI K., TAKEUCHI H., *Copper Extraction by LIX65N in Liquid–Liquid Dispersion System*, Kagaku Kogaku Ronbunshu (Collected Papers of Chemical Engineering, Japanese document), 1985, 11, 349–352.
- [12] YAMAMOTO T., NISHII K., KAWASAKI H., YAMAGUCHI S., *Characteristics of a Small Sized Continuous Disperser with Needle Jet (in Case of Using Two Parallel Needles)*, Atomization (J. ILASS–Japan, Japanese document), 1996, 5, 64–70.
- [13] YAMAMOTO T., KAWASAKI H., KUMAZAWA H., *Generalized Characteristics of Emulsification with Two Different Types of Motionless Mixer*, Atomization (J. ILASS–Japan, Japanese document), 1999, 8, 59–65.
- [14] BERKAMN P.D., CALABRESE R.V., *Drop Sizes Produced by Static Mixers*, AIChE Annual Meeting, paper 27e, Chicago, USA, 1985.
- [15] BERKMAN P.D., CALABRESE R.V., *Dispersion of Viscous Liquids by Turbulent Flow in a Static Mixer*, AIChE J., 1988, 34, 602–609.
- [16] YAMAMOTO T., KUMAZAWA H., *Emulsification of Water–Kerosene Systems with Ramond Supermixer*, Proceedings of the 10th APCChE Congress, 1P-09-018, Kitakyushu, Japan, 2004.
- [17] MIDDLEMAN S., *Drop Size Distributions Produced by Turbulent Pipe Flow of Immiscible Fluids through a Static Mixer*, Ind. Eng. Chem. Process Des. Dev., 1974, 13, 78–83.
- [18] MCMANAMEY W.J., *Sauter Mean and Maximum Drop Diameters of Liquid–Liquid Dispersions in Turbulent Agitated Vessels at Low Dispersed Phase Hold-Up*, Chem. Eng. Sci., 1979, 34, 432–434.
- [19] RAJARATNUM N., *Turbulent Jets*, Developments in Water Science, Vol. 5, Chapt. 2, Elsevier Science, 1976/06.
- [20] SATO K., *Mixing Process in a Jet Mixing Vessel*, Kagaku Kogaku (Memoir of the Society of Chemical Engineers, Japan, Japanese document), 1968, 32, 588–594.
- [21] Chemineer Inc., *Drop Formation of Low-Viscosity Fluids in the Kenics Mixer*, Kenics Static Mixers KTEK Series, KTEK-5, Dayton, USA, 1988.
- [22] YAMAMOTO T., TANAKA M., KAWASAKI H., *Effects of Surfactant Concentration on Drop Sizes in O/W and W/O/W Emulsions*, J. Chem. Eng. Japan, 2003, 36, 963–970.